Contact line dynamics in curtain coating of non-Newtonian liquids

Cite as: Phys. Fluids **33**, 103103 (2021); https://doi.org/10.1063/5.0064467
Submitted: 23 July 2021 • Accepted: 13 September 2021 • Published Online: 06 October 2021

Alireza Mohammad Karim, Wieslaw J. Suszynski, Saswati Pujari, et al.

Physics of Fluids ARTICLE scitation.org/journal/phf

Contact line dynamics in curtain coating of non-Newtonian liquids

Cite as: Phys. Fluids **33**, 103103 (2021); doi: 10.1063/5.0064467
Submitted: 23 July 2021 · Accepted: 13 September 2021 ·
Published Online: 6 October 2021

Alireza Mohammad Karim,[1,2,a)] Wieslaw J. Suszynski,[2] Saswati Pujari,[3] Lorraine F. Francis,[2] and Marcio S. Carvalho[2,4]

AFFILIATIONS

[1]Nanoscience Centre, Department of Engineering, University of Cambridge, 11 J. J. Thomson Avenue, Cambridge CB3 0FF, United Kingdom
[2]Department of Chemical Engineering and Materials Science, University of Minnesota, 421 Washington Ave. SE, Minneapolis, Minnesota 55455, USA
[3]Dow, 400 Arcola Road Collegeville, Pennsylvania 19426, USA
[4]Department of Mechanical Engineering, Pontifícia Universidade Católica do Rio de Janeiro, Rua Marques de São Vicente 225, Gávea, Rio de Janeiro, RJ 22453-900, Brazil

[a)]**Author to whom correspondence should be addressed:** alireza.m.k.2010@gmail.com

ABSTRACT

The rheological characteristics of liquids play an important role in the flow near dynamic contact lines, where the deformation rates are extremely large. The liquid contact line dynamics and the free surface configuration in the curtain coating of polymer solutions were experimentally studied using visualization to determine the effect of two rheological characteristics: shear thinning and extensional thickening. The critical web speeds for heel formation, where the contact line on the moving substrate shifts upstream of the falling curtain, and air entrainment, where the contact line shifts downstream and air bubbles appear, were determined over a range of flow rates. The critical conditions were compared to the behavior observed for a Newtonian liquid. Moreover, the contact line dynamics were described by three dimensionless parameters: the Deborah number, the Ohnesorge number, and the ratio of the web speed to the liquid curtain velocity at the contact line.

I. INTRODUCTION

Curtain coating is used for high-speed precision coating of single-layer and multi-layer films for a variety of applications. During curtain coating, a thin liquid sheet flows vertically downward and is accelerated by gravity over a certain distance before it impinges on the surface of the moving substrate to be coated, as illustrated in Fig. 1(a).[1–4] Coating processes rely on steady dynamic wetting to uniformly deposit a liquid layer onto a moving web. That is, the dynamic contact line (DCL) is stable, located beneath the falling curtain. However, if the substrate speed drops below a critical value, liquid accumulates to form a "heel," and the DCL shifts upstream from the stable location, as sketched in Fig. 1(b). Above a critical substrate speed, the air layer in contact with the substrate is not fully displaced, the flow evolves from steady two-dimensional to unsteady three-dimensional flow,[7–9] and a small amount of air is entrained under the liquid layer [Fig. 1(c)]. Air entrainment degrades film uniformity and product quality, and therefore should always be avoided in coating processes.[10]

In curtain coating, the momentum of the liquid flowing down the curtain creates a high-pressure region near the contact line that helps displace the air layer in contact with the substrate, enabling wetting at higher speeds than observed in other coating methods.[11,12] The delay in air entrainment associated with this high-pressure region is generally referred to as "hydrodynamic assist."[13–16] Experimental observations show that the degree of hydrodynamic assist reaches its maximum (i.e., the largest critical speed) at a specific flow rate, at which the DCL is right beneath the liquid curtain, which leads to a strong hydrodynamic pressure near the DCL as the liquid impacts the substrate.[4,11–13,16,20,21]

In curtain coating, uniform films are only possible in a limited range of operating parameters referred to as the coating window. Traditionally, the curtain coating operating space is defined in terms of two dimensionless parameters: the ratio of the web speed (U_w) to the curtain velocity near the liquid contact line (U) and the Reynolds number—defined as $\mathrm{Re}=\frac{\rho Q}{\mu}$, where Q is the flow rate per unit width,

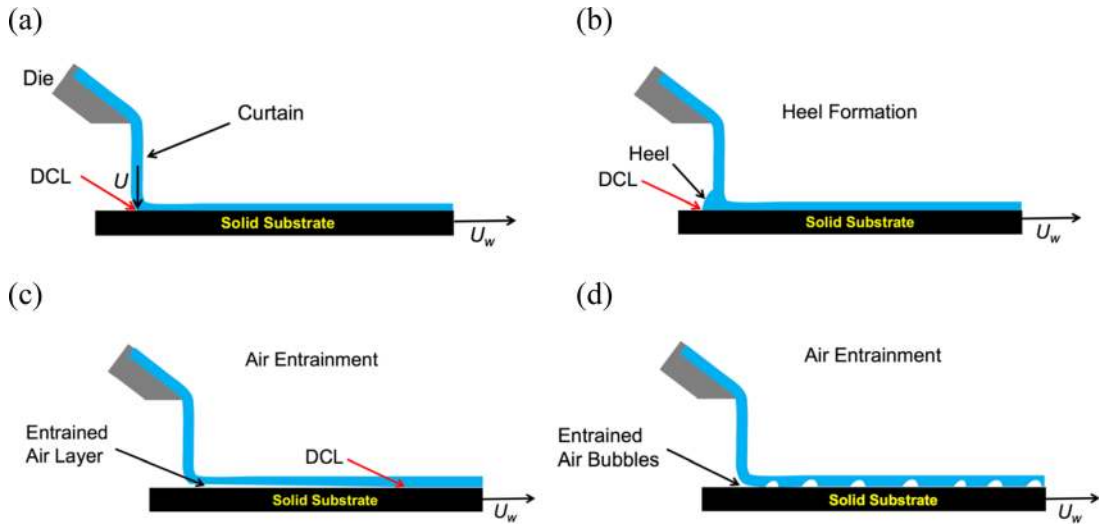

FIG. 1. (a) Schematic of a stable liquid curtain falling with the velocity, U, at the impingement zone on a web moving at speed U_w. (b) Formation of an excess liquid behind the impingement zone. (c) Entrainment of air layer below the coated film. (d) Entrainment of air bubbles below the coated film.

ρ is the liquid density, and μ is the viscosity of the liquid film. For a given liquid and die height, the operating space may also be represented in terms of the web speed U_w and the flow rate Q. One bound on the coating window is set by curtain breakup; the flow rate needs to be above a certain critical value to avoid this phenomenon.[17–19] At each flow rate above this critical value, there is a range of web speeds at which two-dimensional flow occurs. As mentioned above, if the web velocity is not high enough, liquid accumulates in the coating bead to form a heel, and if too high, air entrainment occurs. The boundaries on the coating window also depend on the properties of the liquid.

Marston *et al.*[14] studied the effect of viscosity of Newtonian aqueous solutions of glycerol, with shear viscosity in the range of 97–213 mPa s, on the maximum speed at which air entrainment occurs in a pre-wetted substrate. They have found a significant effect of viscosity on the onset of air entrainment.[14] They have concluded that air entrainment is delayed and occurs at higher speeds as the hydrodynamic assist becomes stronger due to lower viscous drag (i.e., lower viscosity of liquid) or higher inertia (i.e., larger curtain flow rate). Blake *et al.*[13] observed a similar behavior.

Coating liquids are seldom Newtonian. Depending on the liquid formulation, the coating liquids may exhibit shear thinning behavior or present viscoelastic characteristic. Because of the extremely high deformation rate near the contact line, the non-Newtonian behavior may change the force balance in the curtain coating flow that defines the upstream meniscus configuration and dynamic contact line position. Therefore, understanding the relationship between rheological properties of the non-Newtonian liquid and the onset of air entrainment and heel formation is important to define the optimal operating conditions for uniform film production using curtain coating. This relationship has received little attention in the literature and is not well understood.

The effect of rheological behavior on dynamic wetting of a substrate plunging into a liquid bath, i.e., a dip coating process, has been previously studied.[22–30] Wei *et al.*[22] found that, in dip coating, elastic stress enhances viscous bending near the dynamic contact line which promotes air entrainment. Wei *et al.*[23] concluded that viscous bending is reduced as the shear viscosity falls in the region close to the dynamic contact line. Because the flow kinematics in dip coating is very different than that of a curtain coating flow, it is not clear whether the observations can be extended to the case of curtain coating flows. Recently, Charitatos *et al.*[34] developed a hydrodynamic model for wetting failure in a rectangular cavity and showed that wetting failure occurred at higher web velocity in shear thinning liquids and lower velocity in shear thickening liquids. Their modeling results also showed that wetting failure occurs by a common mechanism involving tangential stress balance near the contact line, which governs the thickness of the air phase next to the liquid and hence the capillary-stress gradient that causes air to move away from the contact line.

Here, we experimentally study the effect of shear thinning and extensional thickening (viscoelastic) behavior on the onset of heel formation and air entrainment, which defines the velocity range at a specified flow rate at which a uniform liquid film can be produced. The critical conditions were compared to the behavior observed for Newtonian liquids having similar shear viscosities. This work builds on our past studies of the effect of rheology on curtain breakup.[6,17] Aqueous solutions of xanthan gum (shear thinning liquid films) as well as high-molecular weight polyethylene oxide solutions (extensional thickening liquid films) were used as model liquids in the experiments.

II. EXPERIMENTAL ANALYSIS

A. Materials

1. Newtonian solution

An aqueous solution of polyethylene glycol (PEG, 8000 g/mol) at 20% by weight concentration with 2.77 mM of sodium dodecyl sulfate (SDS) surfactant was used as the Newtonian liquid. The surface tension, σ, was determined with the Wilhelmy plate technique using the tensiometer K 10ST (Krüss). The shear viscosity μ_s was measured with the AR-G2 Rheometer (TA Instruments) based on a Couette cell

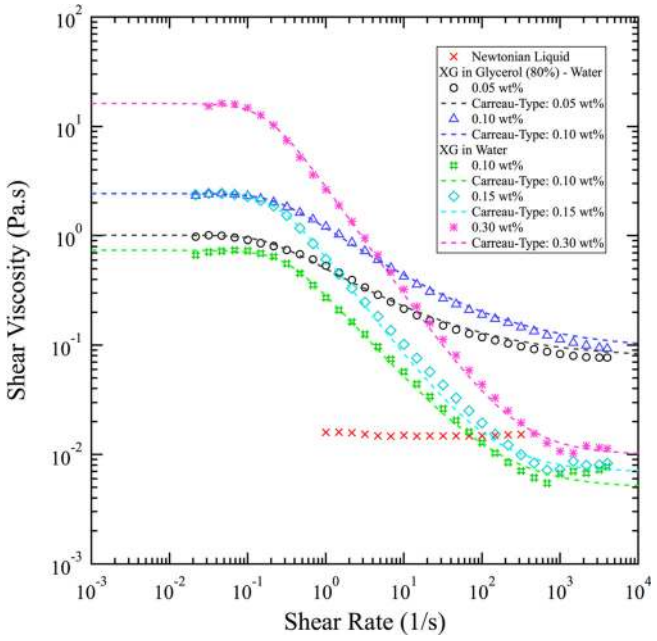

FIG. 2. Viscosity vs shear rate for shear thinning solutions. Some plots in this figure are reproduced with permission from previous study.[6] Reproduced with permission from Karim *et al.*, J. Non-Newtonian Fluid Mech. **263**, 69 (2019). Copyright 2021 Elsevier.

geometry, and the density, ρ, was determined with the Krohne MFC 100 Coriolis type mass flow meter applied in the curtain coating experiment. The physical properties of all solutions used in this work were measured using the same techniques applied in a previous study.[6,17] The PEG/SDS/distilled water solution has Newtonian behavior with a shear viscosity equal to $\mu_s = 19.1$ mPa s (see Fig. 2). The surface tension and density of this solution were $\sigma = 42.6$ mN/m and $\rho = 1028.6\,\mathrm{kg/m^3}$, respectively.

2. Shear thinning solutions

Solutions of xanthan gum in distilled water or glycerol (80 wt. %) water solution were used as the shear thinning liquids. The same procedure was followed to prepare the xanthan gum solutions in a previous study.[6,42] Briefly, xanthan gum powder was dissolved in distilled water or glycerol (80%) aqueous solution. Next, 0.7 mM SDS was added and the solutions were homogenized at a speed of 25 000 rpm for 4 min with a homogenizer (IKA model T 18). The solutions were kept in quiescent condition to remove entrained air bubbles. The physical and rheological properties of these solutions were characterized using methods described in Sec. II A 1 and previous study.[6] Their physical properties are presented in Table I.

The xanthan gum solutions exhibit shear thinning behavior (see Fig. 2). The measurements show that the high shear viscosity, μ_{HS}, i.e., the shear viscosity at the highest shear rate at which viscosity could be measured, is mostly determined by the solvent viscosity. Solutions with different xanthan gum concentrations in the same solvent have almost similar high shear viscosity μ_{HS} and different values for the low shear viscosity μ_{LS}. To characterize the rheological behavior of the shear thinning liquids, the Carreau-type model was employed,[35,36]

$$\mu(\dot{\gamma}) = \mu_{HS} + (\mu_{LS} - \mu_{HS})[1 + (\lambda\dot{\gamma})^2]^{(n-1)/2}. \quad (1)$$

In the Carreau-type constitutive model [Eq. (1)], n is the exponent and λ is the relaxation time that defines the onset of shear thinning behavior.

Xanthan gum solutions do not present strong elastic stress and are usually considered as inelastic liquids.[23,31] The extensional viscosities of the xanthan gum solutions used in this work were measured utilizing the Capillary Breakup Extensional Rheometer (CaBER)[38] and are reported elsewhere.[6] Briefly, liquid filament breakup for aqueous xanthan gum solutions was too rapid to be accurately measured, and the filament thinning of xanthan gum dissolved in 80% glycerol solutions was purely related to the viscous breakup regime.[6] For xanthan gum in glycerol solutions, the extensional viscosity was approximated as 1.3 Pa s for the 0.05% (by weight) xanthan gum in glycerol solution and 4.1 Pa s for the 0.1% (by weight) xanthan gum in glycerol solution.[6] Similar findings have been reported in the literature.[39–41]

3. Extensional thickening solutions

Aqueous solutions of 20% by weight of polyethylene glycol (PEG, 8000 g/mol) and polyethylene oxide (PEO, 4×10^6 or 8×10^6 g/mol) with 2.77 mM of SDS surfactant were used as the extensional thickening liquids.[32] The surface tension of the solutions was reduced by adding a surfactant (2.77 mM of SDS). Small amount of high molecular weight polymer (PEO) powders were dissolved into the PEG (20% w/w)–SDS (2.77 mM) solution to prepare extensional thickening liquids. The physical and rheological properties of these solutions were characterized using methods described in Section II A 1. Results for the set of liquids used in the present study are shown in Table II. Details

TABLE I. Physical properties of shear thinning solutions. Some of the data are reproduced with permission from previous study.[6] Reproduced with permission from Karim *et al.*, J. Non-Newtonian Fluid Mech. **263**, 69 (2019). Copyright 2021 Elsevier.

Xanthan gum (wt. %)	Solvent	Density, ρ (kg/m^3)	Surface tension, σ (mN/m)	Low shear viscosity, μ_{LS} (mPa s)	High shear viscosity, μ_{HS} (mPa s)	λ (s)	n	R^2
0.10	Water	992.0	46.5	740	5	3.28 ± 0.10	0.21 ± 0.02	0.993
0.15	Water	992.7	57.5	2440	7	4.18 ± 0.09	0.07 ± 0.02	0.999
0.30	Water	986.2	58.3	16290	10	5.76 ± 0.35	0.00 ± 0.06	0.996
0.05	Glycerol (80 %)	1197.1	59.0	1010	77	5.61 ± 0.34	0.55 ± 0.01	0.995
0.10	Glycerol (80 %)	1195.3	58.5	2431	93	4.54 ± 0.12	0.50 ± 0.01	0.998

TABLE II. Physical and rheological properties of the extensional thickening solutions.

Concentration of PEO-4 × 10^6 g/mol (wt. %)	Concentration of PEO-8 × 10^6 g/mol (wt. %)	Density, ρ (kg/m^3)	Surface tension, σ (mN/m)	Shear viscosity, μ_0 (mPa s)	Extensional viscosity, μ_e (Pa s)—before experiment	Extensional viscosity, μ_e (Pa s)—after experiment
0	0	1028.6 ± 0.2	42.6	16.0	0.06	0.06
0.08	0	1028.8 ± 0.2	42.0	21.9	109	91.9
0	0.05	1029.2 ± 0.4	42.8	24.3	169	106
0	0.10	1028.9 ± 0.2	43.0	27.9	263	207

on the measurement of extensional viscosity using Capillary Breakup Extensional Rheometer (CaBER) as well as values of the Trouton ratio and relaxation time are provided in the supplementary material. Shear viscosity measurement showed that these solutions present a Boger liquid behavior, the viscosity is almost independent of the shear rate, as shown in Fig. 3.

B. Experimental setup and procedure

The curtain coating experiment was conducted following the procedure detailed in our previous study and is shown schematically in Fig. 4.[17]

The dynamics of the contact line were recorded using a Point Grey camera, with a Navitar Zoom 6000 lens with 0.67X adapter. The contact line was illuminated by a photographic 500 W spotlight. The dynamic contact line was monitored from the bottom of the curtain through the glass roll to observe air entrainment and heel formation at different flow rates and speeds of the glass roll, as indicated in Fig. 4(a). The curtain and deposited film were also recorded with a Photron FASTCAM Ultima APX camera mounted in front of the curtain with a field of view that spanned the width of the curtain, also indicated in Fig. 4(a).

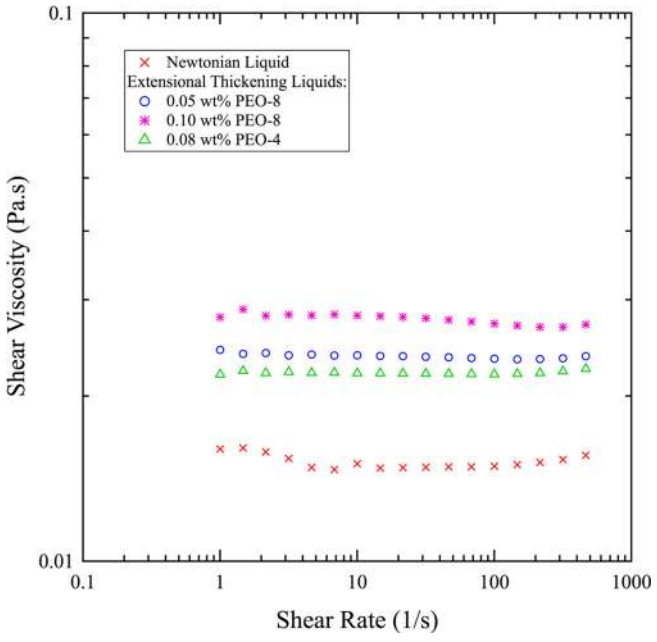

FIG. 3. Shear viscosity vs shear rate of extensional thickening solutions. PEO-8: PEO (8 × 10^6 g/mol); PEO-4: PEO (4 × 10^6 g/mol).

Because liquid is recirculated in the experimental setup, the polymer solution is mechanically degraded during pumping and curtain flow. We ran the setup for five minutes before starting to collect data to make sure the liquid is well mixed, and for no longer than 30 minutes. The shear rheological characteristics of the polymer solutions did not change significantly during the experiments. Some degradation of the extensional thickening solutions was observed, resulting in a drop in the extensional viscosity ranging from 16% to 37%. See Table II and supplementary material.

The range of the flow rates for this study was chosen based on the data reported for the stability of a liquid curtain of these liquid models used in previous studies.[6,17] At each specified flow rate over which the stable liquid curtain could be maintained, the dynamic contact line stability was studied. At each constant flow rate, Q, the speed of the glass roll, U_w, was slowly increased until V-shaped air pocket(s) were observed. The corresponding speed of the glass roll is defined as the critical speed for onset of air entrainment. For the same flow rate, the speed of the glass roll was then decreased slowly until a heel of liquid was observed at any location along the dynamic contact line. The corresponding speed of the glass roll is defined as the critical speed for the onset of heel formation. Due to limitations in the setup, the maximum speed, $U_{w,max}$, the glass roll can achieve in the experiment is 164.2 cm/s.

Figure 5 illustrates the visualization from bottom and front views of the dynamic contact line representing stable dynamic contact line, air entrainment, and heel formation for a Newtonian solution. Figure 5(a) shows the stable dynamic contact line. The presence of V-shaped air pockets along the dynamic contact line reveals air entrainment [Fig. 5(b)]. Heel formation is defined by presence of excess liquid in the upstream side of the coating bead and the position of the dynamic contact line shifted upstream, as shown in Fig. 5(c). Sometimes, a combination of heel formation and air entrainment was observed along the dynamic contact line, as shown in Fig. 5(d).

III. RESULTS AND DISCUSSION

At a constant flow rate, the dynamic contact line is stable between a range of roll speed. The two limits are associated with the following phenomena: the onset of heel formation via the presence of an excess liquid behind the dynamic contact line and the formation of a thin air layer or air bubbles underneath the liquid film. The critical roll speeds associated with these two phenomena were determined here for different flow rates.

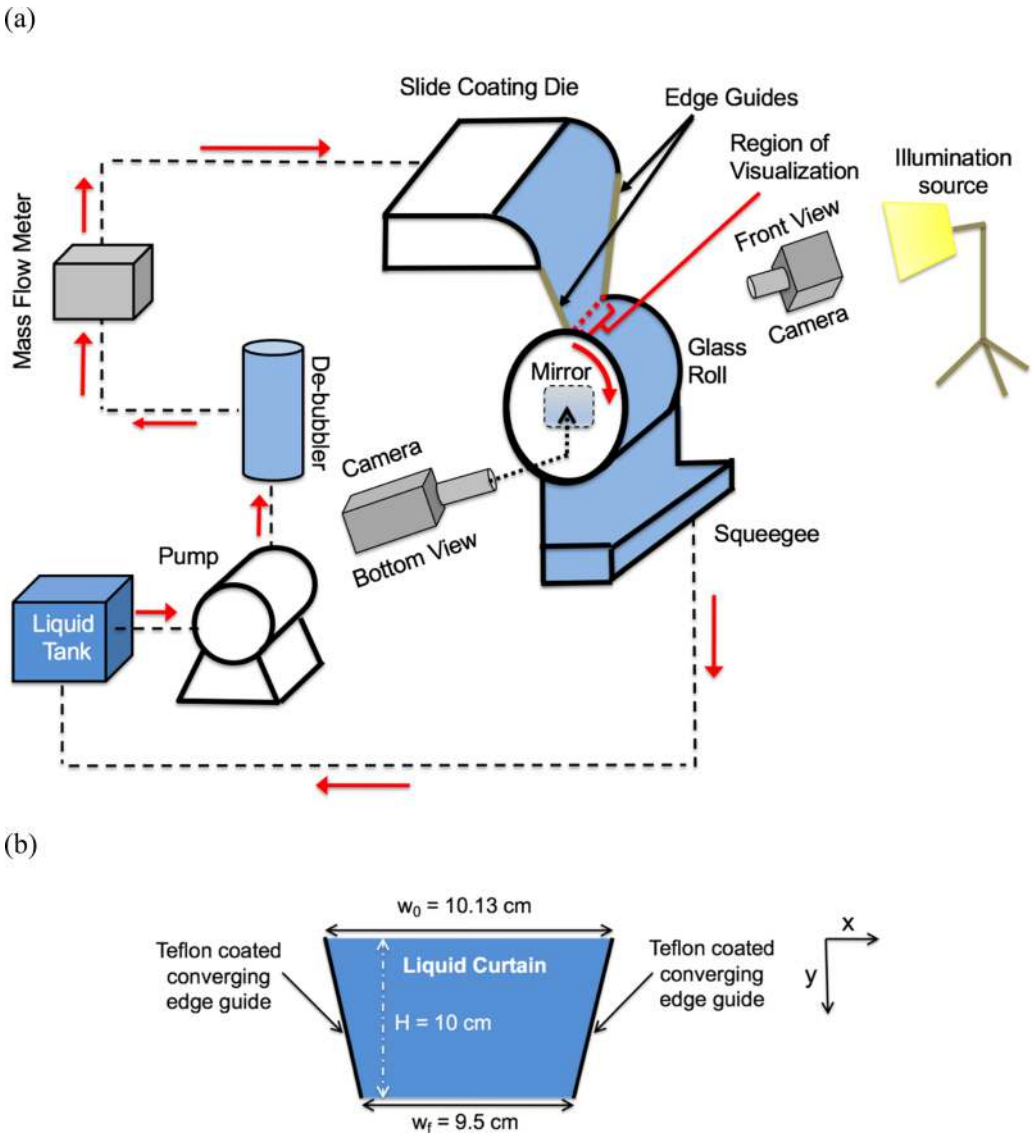

FIG. 4. (a) Schematics of coating and visualization structures. (b) Front view of the stable liquid curtain between two Teflon coated inclined edge guides. *H* is the height of the liquid curtain.

A. Newtonian solution

Figure 6 shows a portion of the coating window for the Newtonian solution. Data were collected at flow rates (Q) higher than the minimum flow rate for a stable curtain. Figure 6 shows the speeds at which heel formation and air entrainment occur at every tested flow rate. The contact line remains stable in between these two values. Based on the previous study on curtain stability,[17] at flow rates below 1.24 cm^2/s, the Newtonian liquid curtain became unstable and broke up; therefore, the dynamic contact line could not be tested. At flow rate above 2 cm^2/s, the liquid contact line becomes unstable: heel formation is observed at every glass roll speed, tested in this study. Therefore, we can define the maximum operable flow rate, Q_{max}, as 2 cm^2/s for this liquid. At flow rates higher than Q_{max}, heel formation combined with air entrainment occurs along the dynamic contact line. A previous study[33] for liquid contact line stability of Newtonian liquids (i.e., glycerol solutions) is consistent with our experimental findings. The coating window of the Newtonian liquid (i.e., 20 wt. % PEG solution) is presented as a reference for comparison with the results obtained for the shear thinning and extensional thickening solutions. The range of Reynolds number ($\mathrm{Re}=\frac{\rho Q}{\mu}$) and capillary number ($\mathrm{Ca}=\frac{\mu_s U_w}{\sigma}$) over which the Newtonian liquid was tested were $8.6 < Re < 12.4$ and $3.7 < Ca < 28.8$, respectively. A previous study[33] was conducted over a similar range of Reynolds number and capillary number as our study as follows: $0.14 < Re < 33.02$ and $0.16 < Ca < 25.07$. The Newtonian solution used has a shear viscosity close to that of the viscoelastic extensional thickening solutions as well as the high shear viscosity of the inelastic shear thinning solutions.

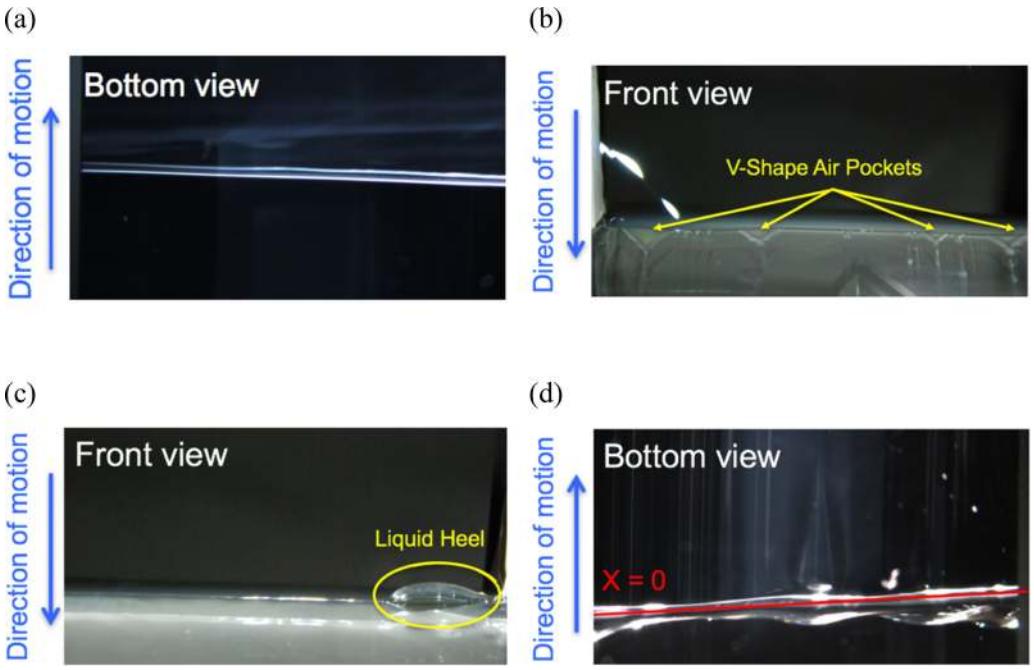

FIG. 5. Visualization of the dynamic contact line for Newtonian solution. (a) Bottom view of a stable dynamic contact line at $U_w = 20$ cm/s and $Q = 13.64$ cm^3/s. (b) Front view of air entrainment (i.e., presence of V-shaped air pockets on glass roller) at $U_w = 38.32$ cm/s and $Q = 13.64$ cm^3/s. (c) Front view of heel formation at $U_w = 9.85$ cm/s and $Q = 13.64$ cm^3/s. (d) Bottom view of a combined air entrainment and heel formation at $U_w = 76.64$ cm/s and $Q = 19.48$ cm^3/s.

B. Shear thinning solutions

In curtain coating, the liquid experiences a large deformation rate near the dynamic contact line. Therefore, the high shear viscosity is expected to play a significant role in determining the onset of air entrainment. Similar to the case of Newtonian liquids, the analysis of dynamic contact line stability for shear thinning liquids was conducted at a flow rate higher than the critical values at which the shear thinning liquid curtains became unstable and broke up. These critical values of the flow rate reported in our previous study[6] were 1.48, 1.08, and 0.86 cm^2/s for the 0.10%, 0.15%, and 0.30% xanthan gum in water, respectively. Moreover, according to this previous work,[6] the critical flow rates for the 0.05% and 0.10% xanthan gum in 80% glycerol were 0.70 and 0.65 cm^2/s, respectively. We first analyzed the behavior of the shear thinning solutions that have a lower viscosity value at high shear rate, i.e., the 0.10%, 0.15%, and 0.30% xanthan gum in water. For these shear thinning solutions, air entrainment was not seen along the liquid contact line up to the maximum possible speed of the glass roll $U_{w,max} = 164.2$ cm/s. Similar findings were also reported by Karim *et al.*[5] The high shear viscosity of xanthan gum solution in water ($\mu_{HS} = 5$–10 mPa s) is close to half of the Newtonian liquid, $\mu_0 \cong 16$ mPa s, which experienced air entrainment at a much lower glass roll speed, $40 \leq U_w \leq 80$ cm/s, at the same range of flow rates, Q. These results reveal that a reduction in high shear viscosity can significantly delay air entrainment. These results are consistent with the observations of Wei *et al.*[23] who studied dynamic wetting in dip coating method (i.e., immersing a vertical cylinder at a controlled constant speed into a pool of non-Newtonian liquid) and Charitatos *et al.*[34] who conducted motivating curtain coating experiments for their modeling work on wetting failure in liquids flowing in rectangular channels. Both Wei *et al.* and Charitatos *et al.* concluded that the reduction in viscous bending is caused by the reduction of shear viscosity of the liquid near the dynamic contact line due the shear thinning behavior.

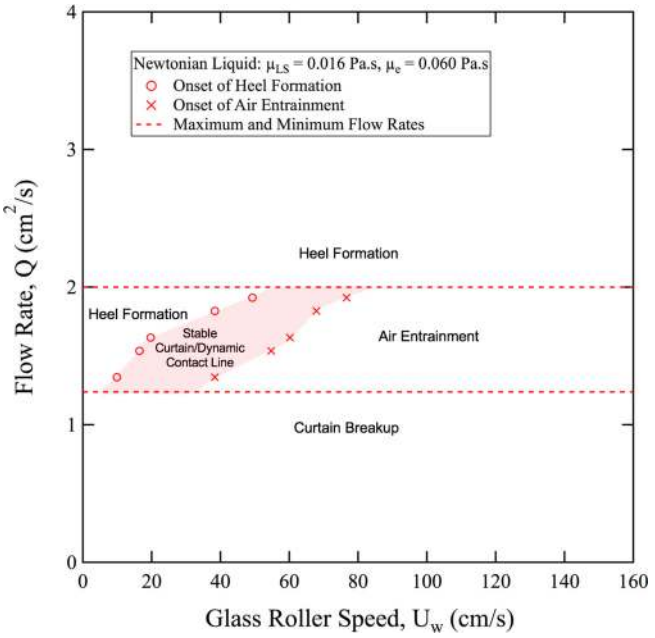

FIG. 6. Onsets of heel formation and air entrainment of the Newtonian solution.

The onset of air entrainment occurs at a critical capillary number ($Ca = \mu_{HS} U_w/\sigma$) at which the apparent contact angle approaches

180°. Shear thinning solutions with low values of high shear viscosity enable higher web speeds keeping the capillary number below the critical value. Moreover, it is important to note that the high shear viscosity, which is the shear viscosity close to the contact line, is the most important parameter of the rheological curve that affects the onset of air entrainment.

Figure 7 shows the critical speeds at every flow rate for the onset of heel formation for xanthan gum solutions in water. As the concentration of the xanthan gum solution increases, which consequently leads to higher viscosity, the onset of heel formation occurs at lower glass roll speeds. This trend becomes stronger for higher flow rates. Again, there is a maximum flow rate, Q_{max}, above which the liquid contact line becomes unstable at any speed of the glass roll. Unlike Newtonian liquids, at $Q > Q_{max}$ only heel formation was seen without any air entrainment at the glass roll speeds tested. The maximum flow rate, Q_{max}, increases as the concentration of xanthan gum and hence the viscosity increase.

Unlike xanthan gum solutions in water, air entrainment was observed in xanthan gum solutions in 80% glycerol, which have higher high shear viscosity. Similar solutions (xanthan gum in 80% glycerol) were also used in a previous study.[37] This is related to the fact that the high shear viscosity of xanthan gum solution in 80% glycerol, $\mu_{HS} = 77$–93 mPa s, is larger than that of xanthan gum solution in water, $\mu_{HS} = 5$–10 mPa s. Figure 8 shows the critical speeds for the onset of air entrainment and the onset of heel formation for these solutions as a function of the imposed flow rate. Though the value of the

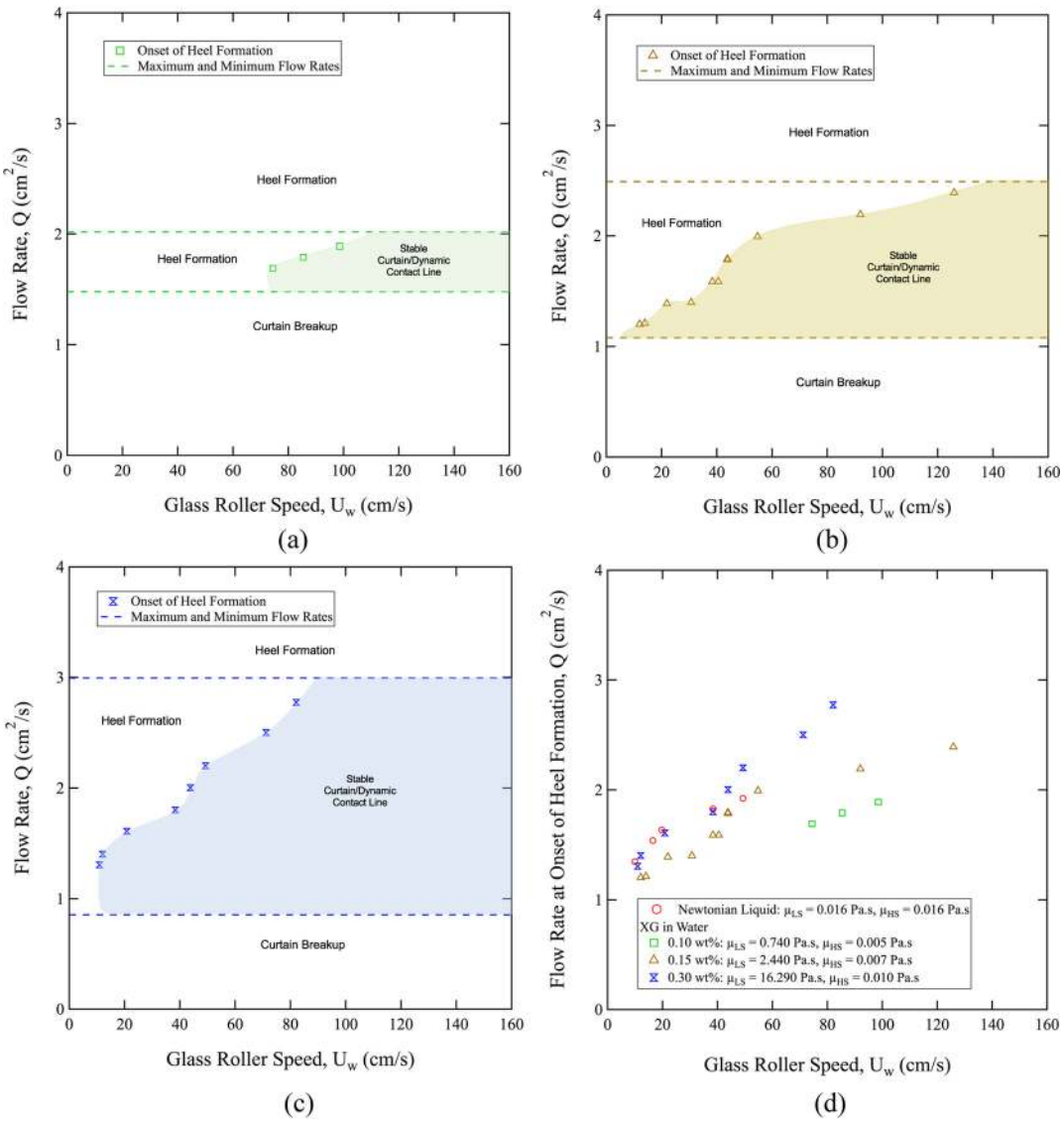

FIG. 7. Shear thinning curtain coating window: (a) 0.10 wt. % xanthan gum in water; (b) 0.15 wt. % xanthan gum in water; (c) 0.30 wt. % XG in water. (d) Comparison of the onset of heel formation for shear thinning solutions in water with a Newtonian liquid.

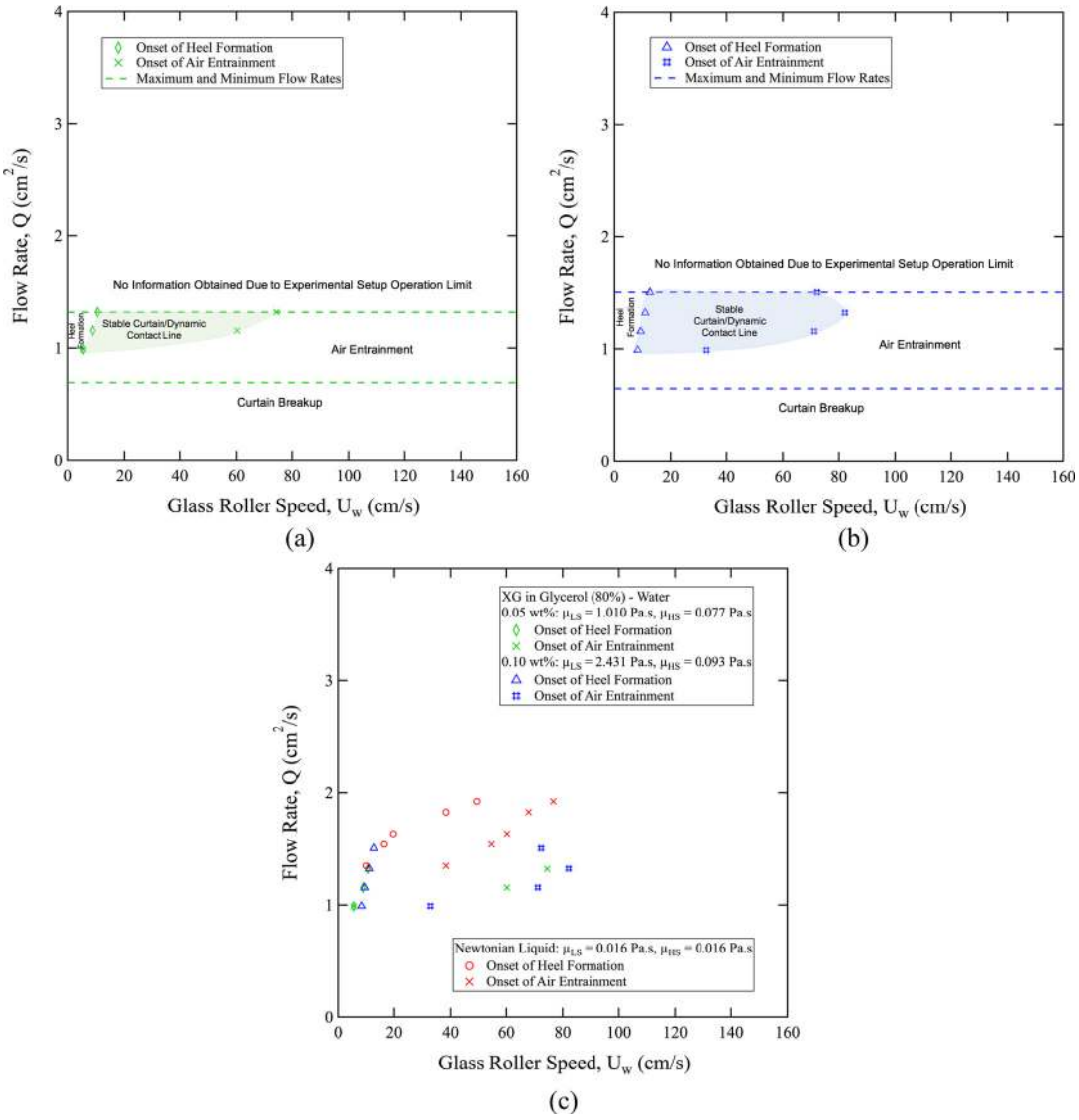

FIG. 8. Shear thinning curtain coating window: (a) 0.05 wt. % xanthan gum in glycerol (80%); (b) 0.10 wt. % xanthan gum in glycerol (80%). (c) Comparison of the onset of air entrainment and heel formation for shear thinning solutions in glycerol with Newtonian liquid. Some plots in this figure are reproduced with permission from previous study.[37] Reproduced with permission from Karim *et al.*, J. Coat. Technol. Res. (published online 2021), Copyright 2021 American Coatings Association.

viscosity of the Newtonian liquid ($\mu_0 \cong 16$ mPa s) is much lower than that of xanthan gum solution in 80% glycerol, $\mu_{HS} \cong 77$–93 mPa s, the onset of air entrainment for xanthan gum solutions in 80% glycerol occurs at higher speeds of the glass roll compared to the onset of air entrainment for the Newtonian solution. This was not expected. For Newtonian liquids, the critical speed above which air entrainment is observed rises as the liquid viscosity falls. The shear thinning behavior of the liquid, which leads to a non-uniform viscosity value throughout the flow, caused a delay in air entrainment even for situations at which the local shear viscosity, occurring at the dynamic contact line, was much higher than that of a Newtonian liquid. Considering the web velocity, U_w, and the volumetric flow rate per unit width, Q, the coated film thickness, t_{film}, can be determined by $t_{film} = Q/U_w$. Therefore, the range of average shear rates, $\dot{\gamma}$, in the viscous boundary layer near the dynamic contact line was estimated as follows:

$$\dot{\gamma} = \frac{U_w}{t_{film}}. \tag{2}$$

Table III presents the range of shear rates near the dynamic contact line for shear thinning liquids used in this study. The range of tested shear rates near the dynamic contact line was covered in the rheological data presented earlier.

The onset of heel formation with the xanthan gum in 80% glycerol–water solutions was close to that observed with the

TABLE III. The range of shear rates near the dynamic contact line for shear thinning solutions.

Xanthan gum (wt. %)	Solvent	Shear rate, $\dot{\gamma}$ (1/s)
0.10	Water	3280–15 940
0.15	Water	121–22 430
0.30	Water	91–20 660
0.05	Glycerol (80%)	30–4200
0.10	Glycerol (80%)	68–5100

Newtonian solution. According to the range of shear rates considered in this study, as reported in Table III, we could see that the most relevant parameter of the rheological curves of the shear thinning solutions is the high shear range; so, we can expect to obtain similar results with Newtonian liquids with shear viscosities equivalent to μ_{HS}.

C. Extensional thickening solutions

The stability of the dynamic contact line was studied at flow rates higher than the minimum flow rate needed for curtain stability. These critical values of the flow rate were reported in our previous study:[6] 0.86, 0.32, and 0.77 cm^2/s for the 0.05%, 0.08%, and 0.10% PEO, respectively. Unlike the inelastic Newtonian liquid, air entrainment was observed at every glass roll speed and flow rate tested for all extensional thickening liquids, even though both extensional thickening and Newtonian liquids have similar shear viscosity. This behavior is related to the strong destabilizing effect of high stresses associated with the high extensional viscosity near the dynamic liquid contact line. Figure 9 shows images of the unstable dynamic contact line for 0.08% PEO (4 million g/mol) solution at $Q_{max} \sim 1.55\ cm^2/s$ at different speeds of the glass roll. At the lower range of roll speed, small V-shaped air pockets formed trains of air bubbles on the liquid film deposited on the glass roll [see Figs. 9(a)–9(e)]. As the glass roll speed further increases, the V-shaped air pockets start to merge and combine to form larger V-shaped air pockets [see Figs. 9(f)–9(h)]. It is also to be noted that at low flow rates and at low roll speeds, an oscillation of the position of the dynamic contact line may occur leading to a coating defect known as barring, i.e., wave shape of the liquid film in the down-web direction (see Fig. 10).

Previous studies[22,23] also confirmed that the elastic stress of a viscoelastic liquid enhances the curvature near the dynamic contact line, which promotes air entrainment. However, they concluded that the effect of elasticity on enhancing the curvature near the dynamic contact line is weak. Our experimental results show that elasticity has a much stronger effect on enhancing the curvature close to the dynamic contact line. The reason for this difference may be attributed to the larger value of Weissenberg number in our experiments. The Weissenberg number is defined as $Wi = \lambda U/a$, where λ is the relaxation time of the viscoelastic liquid; U is the roll velocity; and a is the capillary length, $a = \sqrt{\sigma/\rho g}$. Weissenberg number of viscoelastic liquids used in our study are $Wi \sim 1.09$–1.66 which is much larger than its value in previous studies, $Wi \sim 10^{-5}$–10^{-4}.[22] Although the shear viscosity of extensional thickening liquids is very low, air entrainment occurred at any speed. Therefore, this finding reveals the fact that extensional viscosity plays an important role in determining

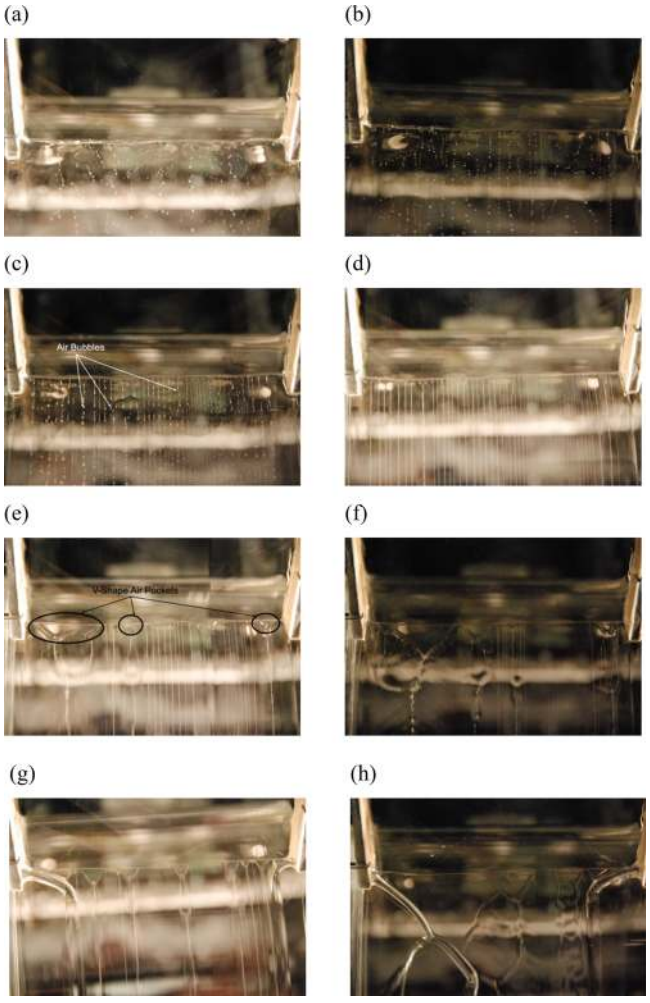

FIG. 9. Dynamic contact line pictures for 0.08% PEO (4×10^6 g/mol) + PEG solution for the flow rate, $Q = 1.55\ cm^2/s$, at glass roll speeds: (a) $U_w \sim 11$ cm/s, (b) $U_w \sim 16.4$ cm/s, (c) $U_w \sim 21.9$ cm/s, (d) $U_w \sim 43.8$ cm/s, (e) $U_w \sim 65.7$ cm/s, (f) $U_w \sim 87.6$ cm/s, (g) $U_w \sim 109.5$ cm/s, (h) $U_w \sim 131.4$ cm/s.

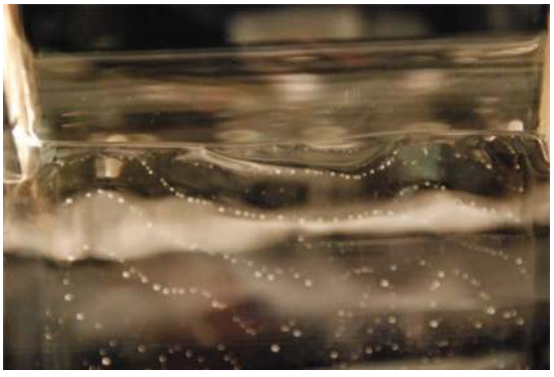

FIG. 10. Barring on the liquid film coated on the substrate at $Q \sim 1.18\ cm^2/s$ and at $U_w \sim 11$ cm/s.

the stability of the dynamic contact line related to the onset of air entrainment.

Figure 11 presents the critical roll speed at the onset of heel formation as a function of flow rates. All the liquids presented similar values, indicating the extensional behavior is not relevant to the dynamics of heel formation. Considering the experimental results obtained for the stability of the dynamic contact line of the extensional thickening solutions, we could assume that extensional viscosity could cause instability along the dynamic contact line at any contact line velocity either via the presence of air entrainment or heel formation.

D. Dimensional analysis

The stability of the dynamic contact line in curtain coating is a function of several physical properties and flow parameters: flow rate, density, rheological behavior such as shear and extensional viscosities and relaxation time, curtain velocity near the dynamic contact line, as well as the web speed. These variables can be combined in different dimensionless parameters. As the results presented in Sec. III C show, it is important to note that both shear and extensional viscosities play a significant role in determining the stability of the dynamic contact line.

Figure 12 presents the onset of heel formation for the liquids tested in this study as a function of three dimensionless numbers: Deborah number, *De*; Ohnesorge number, *Oh*; and the speed ratio, $\hat{u}$. The Deborah number is the ratio of the relaxation time, λ, to the characteristic flow time, $T^* = \frac{t_{film}}{U_w}$, in which t_{film} is the coated film thickness and U_w is the web speed as follows:

$$De = \frac{\lambda}{T^*}. \tag{3}$$

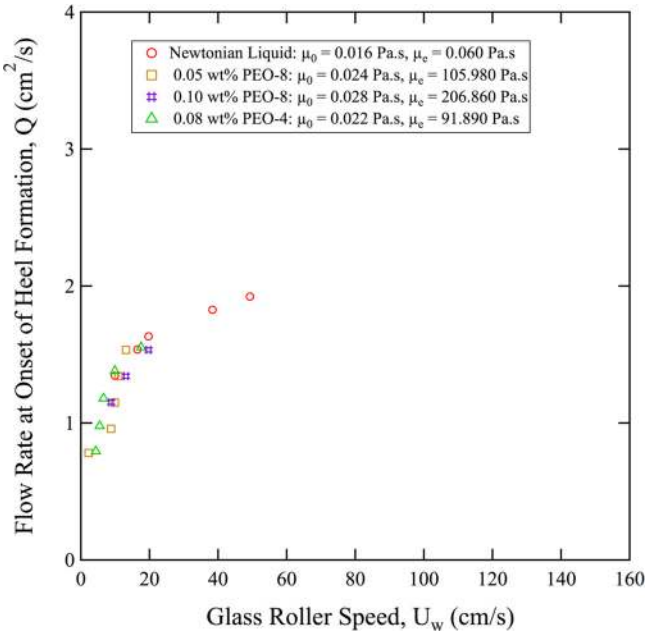

FIG. 11. Onset of heel formation for extensional thickening solutions. PEO-8: PEO (8×10^6 g/mol); PEO-4: PEO (4×10^6 g/mol).

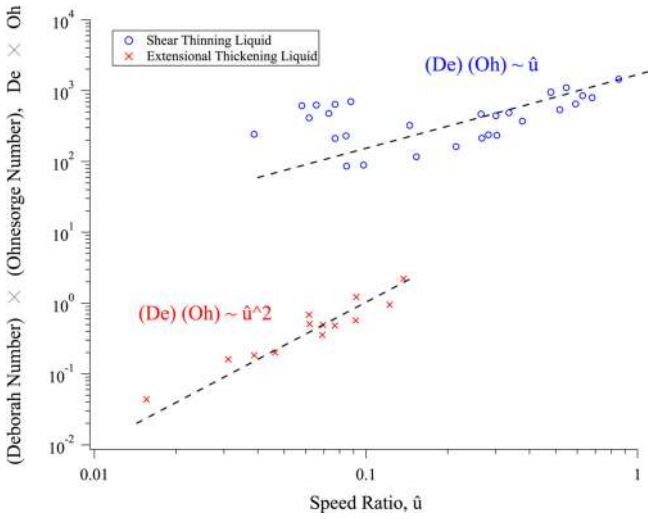

FIG. 12. Plot of $De \times Oh = \lambda \mu^* U_w / \left(t_{film} \sqrt{\rho \sigma t_{film}} \right)$ vs speed ratio, $\hat{u} = U_w / U$, to describe the instability of the dynamic contact line due to the onset of heel formation in curtain coating of liquid films exhibiting shear thinning and viscoelastic behavior.

The Ohnesorge number is the ratio balance of shear, inertia, and capillary forces given by

$$Oh = \frac{\mu^*}{\sqrt{\rho \sigma t_{film}}}. \tag{4}$$

The characteristic viscosity, $\mu^* = \mu(\dot{\gamma}^*)$, is defined as the shear viscosity at the characteristic shear rate, $\dot{\gamma}^* = \frac{U_w}{t_{film}}$.

The speed ratio, $\hat{u}$, is defined as the ratio of the web speed, U_w, and the curtain velocity, U, at the impingement zone as follows:

$$\hat{u} = \frac{U_w}{U}. \tag{5}$$

The curtain velocity at the impingement zone is evaluated assuming that the liquid accelerates as a free fall as follows:

$$U = \left[U_{exit}^2 + 2 g H \right]^{1/2}, \tag{6}$$

where H is the height of the curtain, U_{exit} is the liquid velocity as it exits the die, and g is the gravitational acceleration.

The dimensionless analysis performed for the instability of the dynamic contact line caused by the onset of heel formation on the liquid models investigated in this study (i.e., shear thinning and viscoelastic) reveal that they all follow a power law relation between $(De \times Oh)$ and speed ratio $(De \times Oh \sim \hat{u}^N)$ in which N is the exponent. Shear thinning inelastic liquids follow a linear $(N = 1)$ relation whereas the extensional thickening (viscoelastic liquid) models follow a square power law $(N = 2)$.

IV. FINAL REMARKS

Successful operation in curtain coating processes is directly associated with the flow configuration near the dynamic contact line where the liquid wets the substrate. High-speed coating is possible if the liquid contact line is located right underneath the falling curtain

such that the liquid momentum helps to squeeze out the air layer in contact with the substrate, delaying the onset of air entrainment.

The effect of rheological properties of complex liquids on the stability of the dynamic liquid contact line in a curtain coating process was studied experimentally using a slide die generated curtain coating setup. The critical conditions at which the dynamic liquid contact line becomes unstable were determined by examining the onset of air entrainment and heel formation along the impingement zone. Extensional thickening (i.e., viscoelastic) liquid films with different extensional viscosity and shear thinning liquids with different low shear and high shear viscosities were investigated in this study. The liquid extensional viscosity presents a strong destabilizing effect on the dynamic contact line, promoting the onset of air entrainment at any glass roller speed (i.e., contact line speed) at which the curtain coating experiments were conducted. Moreover, the high shear viscosity in shear thinning liquid films reveals a substantial stabilizing role on the dynamic liquid contact line by delaying the onset of air entrainment.

These findings show that both shear viscosity and the liquid extensional viscosity play a significant role in determining the dynamics of the liquid contact line. The significant reduction in viscous bending caused by a small reduction in the shear viscosity strongly delays the emergence of air entrainment. Comparison of shear thinning solutions with their corresponding base Newtonian solutions proves the fact that local high shear viscosity plays a prominent role in the onset of air entrainment. The presence of air entrainment at any contact line speed for the extensional thickening liquid films reveals the destabilizing effect of the extensional viscosity along the dynamic contact line via promoting a large curvature near the dynamic contact line. Furthermore, dimensionless analysis on the experimental data shows physical evidence on the effect of local high shear viscosity on the emergence of heel formation along the dynamic contact line.

The low shear viscosity in shear thinning liquid films represents a stabilizing effect on the dynamic liquid contact line by delaying the onset of heel formation. Moreover, it was found that in the case of shear thinning liquids, the local shear viscosity, described by the local shear rate of strain evaluated by the web speed and the coated liquid film thickness on the web, is the true shear viscosity of the shear thinning liquid which determines the stability of the liquid contact line.

Moreover, the contact line dynamics of the falling liquid film on the web when heel formation starts was studied by three dimensionless parameters: the Deborah number, De; the Ohnesorge number, Oh; and the speed ratio, $\hat{u}$. Contact line instability due to the onset of the heel formation for non-Newtonian liquids follows a simple power law relation ($De \times Oh \sim \hat{u}^N$). Furthermore, dimensionless analysis shows that shear thinning liquids follow a linear power law ($De \times Oh \sim \hat{u}$) as compared to extensional thickening liquids that follow the power-2 law ($De \times Oh \sim \hat{u}^2$) to describe the onset of heel formation in the curtain coating process.

SUPPLEMENTARY MATERIAL

See the supplementary material for complete details on the measurement of extensional viscosity of viscoelastic liquids used in this study.

ACKNOWLEDGMENTS

We gratefully acknowledge the financial support from Dow for this research.

AUTHOR DECLARATIONS

Conflict of Interest

The authors have no conflicts to disclose.

DATA AVAILABILITY

The data that support the findings of this study are available from the corresponding author upon reasonable request.

REFERENCES

[1]D. R. Brown, "A study of the behaviour of a thin sheet of moving liquid," J. Fluid Mech. **10**, 297–305 (1961).
[2]D. J. Hughes, "Method for simultaneously applying a plurality of coated layers by forming a stable multilayer free falling vertical curtain" U.S. patent 3508947 (28 April 1970).
[3]T. D. Blake, R. Dobson, G. N. Batts, and W. J. Harrison, "Coating processes" U.S. patent 5391401 (21 February 1995).
[4]T. D. Blake, R. A. Dobson, and K. J. Ruschak, "Wetting at high capillary numbers," J. Colloid Interface Sci. **279**, 198–205 (2004).
[5]A. Mohammad Karim, W. J. Suszynski, S. Pujari, L. F. Francis, and M. S. Carvalho, "Delaying breakup and avoiding air entrainment in curtain coating using a two-layer liquid structure," Chem. Eng. Sci. **213**, 115376 (2020).
[6]A. Mohammad Karim, W. J. Suszynski, W. B. Griffith, S. Pujari, L. F. Francis, and M. S. Carvalho, "Effect of rheological properties of shear thinning liquids on curtain stability," J. Non-Newtonian Fluid Mech. **263**, 69–76 (2019).
[7]R. Burley and B. S. Kennedy, "An experimental study of air entrainment at a solid/liquid/gas interface," Chem. Eng. Sci. **31**(10), 901–911 (1976).
[8]T. D. Blake and K. J. Ruschak, "A maximum speed of wetting," Nature **282**, 489–491 (1979).
[9]E. Vandre, M. S. Carvalho, and S. Kumar, "Characteristics of air entrainment during dynamic wetting failure along a planar substrate," J Fluid Mech. **747**, 119–140 (2014).
[10]S. J. Weinstein and K. J. Ruschak, "Coating flows," Annu. Rev. Fluid Mech. **36**(1), 29–53 (2004).
[11]T. D. Blake, M. Bracke, and Y. D. Shikhmurzaev, "Experimental evidence of nonlocal hydrodynamic influence on the dynamic contact angle," Phys. Fluids **11**(8), 1995 (1999).
[12]M. Yamamura, "Assisted dynamic wetting in liquid coatings," Colloids Surf. A **311**, 55–60 (2007).
[13]T. D. Blake, A. Clarke, and K. J. Ruschak, "Hydrodynamic assist of dynamic wetting," AIChE J. **40**, 229–242 (1994).
[14]J. O. Marston, M. J. H. Simmons, and S. P. Decent, "Influence of viscosity and impingement speed on intense hydrodynamic assist in curtain coating," Exp. Fluids **42**, 483–488 (2007).
[15]J. O. Marston, M. J. H. Simmons, S. P. Decent, and S. P. Kirk, "Influence of the flow field in curtain coating onto pre-wet substrates," Phys. Fluids **18**, 112102 (2006).
[16]K. Miyamoto and K. Katagiri, "Curtain coating," in *Liquid Film Coating: Scientific Principles and Their Technological Implications*, edited by S. F. Kistler and P. M. Schweizer (Springer, 1997).
[17]A. Mohammad Karim, W. J. Suszynski, W. B. Griffith, S. Pujari, L. F. Francis, and M. S. Carvalho, "Effect of viscoelasticity on stability of liquid curtain," J. Non-Newtonian Fluid Mech. **257**, 83–94 (2018).
[18]A. Mohammad Karim, W. J. Suszynski, L. F. Francis, and M. S. Carvalho, "Effect of viscosity on liquid curtain stability," AIChE J. **64**(4), 1448–1457 (2018).
[19]M. Becerra and M. S. Carvalho, "Stability of viscoelastic liquid curtain," Chem. Eng. Process. **50**, 445–449 (2011).
[20]M. Yamamura, S. Suematsu, T. Kajiwara, and K. Adachi, "Experimental investigation of air entrainment in a vertical liquid jet flowing down onto a rotating roll," Chem. Eng. Sci. **55**(5), 931–942 (2000).
[21]C. Y. Liu, E. Vandre, M. S. Carvalho, and S. Kumar, "Dynamic wetting failure in surfactant solutions," J. Fluid Mech. **789**, 285–309 (2016).
[22]Y. Wei, G. K. Seevaratnam, S. Garoff, E. Rame, and L. M. Walker, "Dynamic wetting of Boger fluids," J. Colloid Interface Sci. **313**, 274–280 (2007).

[23]Y. Wei, E. Rame, L. M. Walker, and S. Garoff, "Dynamic wetting with viscous Newtonian and non-Newtonian fluids," J. Phys.: Condens. Matter **21**, 464126 (2009).
[24]A. Mohammad Karim, S. H. Davis, and H. P. Kavehpour, "Forced versus spontaneous spreading of liquids," Langmuir **32**, 10153–10158 (2016).
[25]A. Mohammad Karim, "Parametric study of liquid contact line dynamics: Adhesion vs. hydrodynamics," Ph.D. thesis (UCLA, 2015).
[26]H. P. Kavehpour, A. Mohammad Karim, J. P. Rothstein, and S. Davis, "Laws of spreading: When hydrodynamic equations are not enough," in 70th Annual Meeting of the Fluid Dynamics Division of the American Physical Society, Denver, CO (2017).
[27]A. Mohammad Karim and H. P. Kavehpour, "Laws of spreading: Why Tanner, Hoffman, Voinov, Cox and de Gennes were wrong, generally speaking," in 67th Annual Meeting of the Fluid Dynamics Division of the American Physical Society, San Francisco, CA (2014).
[28]A. Mohammad Karim, J. P. Rothstein, and H. P. Kavehpour, "Experimental study of dynamic contact angles on rough hydrophobic surfaces," J. Colloid Interface Sci. **513**, 658–665 (2018).
[29]A. Mohammad Karim and H. P. Kavehpour, "Dynamics of spreading on ultra-hydrophobic surfaces," J. Coat. Technol. Res. **12**, 959–964 (2015).
[30]A. Mohammad Karim and H. P. Kavehpour, "Effect of viscous force on dynamic contact angle measurement using Wilhelmy plate method," Colloids Surf. A **548**, 54–60 (2018).
[31]G. K. Seevaratnam, Y. Sue, E. Rame, L. M. Walker, and S. Garoff, "Dynamic wetting of shear thinning fluids," Phys. Fluids **19**, 012103 (2007).
[32]P. Dontula, C. W. Macosko, and L. E. Scriven, "Model elastic liquids with water-soluble polymers," AIChE J. **44**(6), 1247–1255 (1998).
[33]J. O. Marston, S. P. Decent, and M. J. H. Simmons, "Hysteresis and non-uniqueness in the speed of the onset of instability in curtain coating," J. Fluid Mech. **569**, 349–363 (2006).
[34]V. W. J. Charitatos, M. S. Carvalho, and S. Kumar, "Dynamic wetting failure in shear-thinning and shear-thickening liquids," J. Fluid Mech. **892**, A1 (2020).
[35]R. B. Bird, "Useful non-Newtonian models," Annu. Rev. Fluid Mech. **8**, 13–34 (1976).
[36]P. J. Carreau, D. D. Kee, and M. Daroux, "An analysis of the viscous behaviour of polymeric solutions," Can. J. Chem. Eng. **57**(2), 135–140 (1979).
[37]A. Mohammad Karim, W. J. Suszynski, and S. Pujari, "Liquid film stability and contact line dynamics of emulsion liquid films in curtain coating process," J. Coat. Technol. Res. (published online 2021).
[38]G. H. McKinley and A. Tripathi, "How to extract the Newtonian viscosity from capillary breakup measurements in a filament rheometer," J. Rheol. **44**(3), 653–671 (2000).
[39]M. Khagram, R. K. Gupta, and T. Sridhar, "Extensional flow of xanthan gum solutions," J. Rheol. **29**, 191–207 (1985).
[40]J. R. Stokes, L. J. W. Graham, N. J. Lawson, and D. V. Boger, "Swirling flow of viscoelastic fluids. Part 1. Interaction between inertia and elasticity," J. Fluid Mech. **429**, 67–153 (2001).
[41]S. Migliozzi, L. Mazzei, and P. Angeli, "Viscoelastic flow instabilities in static mixers: Onset and effect on the mixing efficiency," Phys. Fluids **33**, 013104 (2021).
[42]A. Mohammad Karim, "Experimental dynamics of Newtonian and non-Newtonian droplets impacting liquid surface with different rheology," Phys. Fluids **32**, 043102 (2020).